AD-A096 722   TERRA TEK INC SALT LAKE CITY UT   F/G 8/7
               EFFECT OF SHOCK LOADING ON ROCK PROPERTIES AND IN SITU STATES.(U)
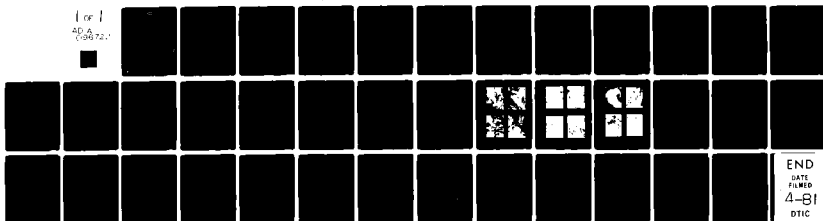   JUN 80   S W BUTTERS, J W LACOMB   DNA001-78-C-0395
UNCLASSIFIED   TR-79-25   DNA-5380T   NL

1 OF 1
AD A
096722

END
DATE
FILMED
4-81
DTIC

LEVEL II

DNA 5380T

EFFECT OF SHOCK LOADING ON ROCK PROPERTIES AND IN SITU STATES

AD A096722

Terra Tek, Inc.
420 Wakara Way
Salt Lake City, Utah 84108

1 June 1980

Topical Report for Period 7 September 1978—1 June 1980

CONTRACT No. DNA 001-78-C-0395

DTIC
SELECTED
MAR 24 1981

F

DTIC FILE COPY

Prepared for

Director

DEFENSE NUCLEAR AGENCY

Washington, D. C. 20305

81 3 24 051

SECURITY CLASSIFICATION OF THIS PAGE (When Data Entered)

REPORT DOCUMENTATION PAGE		READ INSTRUCTIONS BEFORE COMPLETING FORM
1. REPORT NUMBER DNA 5380T	2. GOVT ACCESSION NO. AD-A096 722	3. RECIPIENT'S CATALOG NUMBER
4. TITLE (and Subtitle) EFFECT OF SHOCK LOADING ON ROCK PROPERTIES AND IN SITU STATES.		5. TYPE OF REPORT & PERIOD COVERED Topical Report for Period 7 Sep 78—1 Jun 80
		6. PERFORMING ORG. REPORT NUMBER TR-79-25
7. AUTHOR(s) S. W. Butters J. W. LaComb		8. CONTRACT OR GRANT NUMBER(s) DNA 001-78-C-0395
9. PERFORMING ORGANIZATION NAME AND ADDRESS Terra Tek, Inc. 420 Wakara Way Salt Lake City, Utah 84108		10. PROGRAM ELEMENT PROJECT, TASK AREA & WORK UNIT NUMBERS Subtask J45GAXYX973-10
11. CONTROLLING OFFICE NAME AND ADDRESS Director Defense Nuclear Agency Washington, D.C. 20305		12. REPORT DATE 1 June 1980
		13. NUMBER OF PAGES 38
14. MONITORING AGENCY NAME & ADDRESS(if different from Controlling Office)		15. SECURITY CLASS (of this report) UNCLASSIFIED
		15a. DECLASSIFICATION DOWNGRADING SCHEDULE

16. DISTRIBUTION STATEMENT (of this Report)

Approved for public release; distribution unlimited.

17. DISTRIBUTION STATEMENT (of the abstract entered in Block 20, if different from Report)

18. SUPPLEMENTARY NOTES

This work sponsored by the Defense Nuclear Agency under RDT&E RMSS Code
K400078462 J45GAXYX97310 H2590D.

19. KEY WORDS (Continue on reverse side if necessary and identify by block number)

In situ stress   Air void content
Ultrasonic velocity   Permanent compaction
Triaxial compression   Peak radial stress

20. ABSTRACT (Continue on reverse side if necessary and identify by block number)

In situ characteristics of geological materials are a function of the mineral and chemical composition, physical properties such as porosity and moisture content, and in situ stress state. The material characteristics or behavior can be altered by changes in the above mentioned parameters or by changing the stress history of the material. Very little is known, however, about the latter and especially shock wave induced stress changes. The Nevada Test Site nuclear test program presented an opportunity to study the changes

DD FORM 1473   EDITION OF 1 NOV 55 IS OBSOLETE

UNCLASSIFIED

20. ABSTRACT (Continued)

in ash-fall tuff material resulting from shock waves ranging in magnitude from
approximately 100 MPa to 1000 MPa.

Comparisons are made of the geology, physical and mechanical properties,
geophysical properties, and geomechanical properties of the tuff media, before
and after a nuclear event. The results indicate changes in the physical and
mechanical properties (i.e. stress-volume response, shear strengths, ultra-
sonic velocities), geophysical properties (seismic velocities) and geomechanical
properties (*in situ* stresses). Little change was noticeable in the geology
except for some indication of horizontal movement in small, tight discontinuous
fractures.

PREFACE

1

TABLE OF CONTENTS

LIST OF ILLUSTRATIONS

LIST OF TABLES

INTRODUCTION

Rock material characteristics and behavior can be altered by pressure, temperature, chemistry, and changes in microstructure, saturation, porosity, etc. Of interest are alterations resulting from man induced activities such as mining, oil and gas retrieval and shock induced stress waves. The Nevada Test Site nuclear test program has presented an opportunity to study changes in ash-fall tuff material resulting from the latter -- shock waves.

Planning an underground nuclear event requires information on select geologic locations on a detailed scale not typically required in other geologic related activities. Because of new nuclear test configurations, a recent detailed review has been conducted on materials both before and after the rock material had been subjected to significant stress waves and displacements from a nuclear event. That is, the Dining Car nuclear event media had been thoroughly characterized preshot and was subsequently characterized postshot in preparation for another nearby nuclear event, the U12e.20.

This report summarizes the examination of changes in geologic structures such as faults, joints, etc., physical properties (density, moisture content, gas filled porosity and shear strength), geophysical properties (seismic velocity) and geomechanical properties (*in situ* stress) as a function of the shock wave intensity (i.e. peak radial stress), which varied from about 100 MPa to 1000 MPa.

The information obtained and compiled is a joint effort of several agencies. The Defense Nuclear Agency Field Command Office was responsible

for overall control of the site characterization program with Mr. J. W. LaComb directing the activities. The United States Geological Survey, Special Projects Branch (Denver), obtained the geological, geophysical and geomechanical data while Terra Tek, Inc. (Salt Lake City) supplied the physical properties data.

The data and discussions will be presented in individual sections on geology, physical properties, geophysical properties and geomechanical properties followed by overall conclusions.

SECTION I

GEOLOGY

The Dining Car nuclear test area is located in an ash-fall tuff
approximately 400 meters below the surface and approximately 200 meters
above the Paleozoic rocks in the Rainier Mesa at the Nevada Test Site,
see Figure 1. The water table is approximately 1000 meters below the
surface. The overburden consists of a cap rock (150 meters thick) and
approximately 250 meters of ash-flow and ash-fall tuff with the ash-flow
tuff overlying the ash-fall tuff. The Dining Car area and U12e.20 area
(media characterized for a nuclear event after the Dining Car event)
consist of a thick-bedded to massive zeolitized calcalkaline and peral-
kaline ash-fall tuff with minor amounts of reworked calcalkaline ash-fall
tuff.

The Dining Car complex and associated drill holes are shown in Figure
2. Post-Dining Car drifts (re-entry drifts and U12e.20 drifts) and drill
holes are shown in Figure 3; dashed lines indicate pre-Dining Car con-
figuration. Figure 4 shows the peak radial stresses due to the Dining Car
event.

Effects of the Dining Car Event: The Dining Car re-entry drifts and
U12e.20 drifts provided an opportunity to observe changes in the pre-
Dining Car geology. No bedding plane shifts or fault movements were noted.
However, it must be pointed out that the Dining Car site was not structurally
complex and, therefore, no faults were encountered that were mapped pre-
Dining Car. Small, tight and discontinuous fractures are present in the
U12e.20 drifts and some show evidence of horizontal movement. Even though
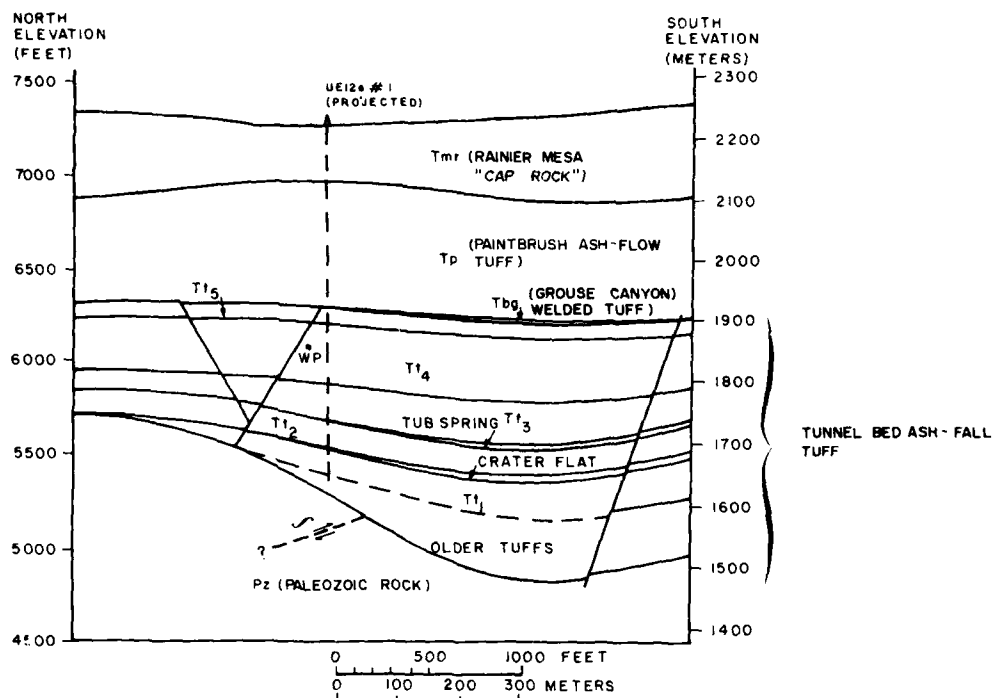
Figure 1a. Approximate north-south cross-section of the Dining Car site.
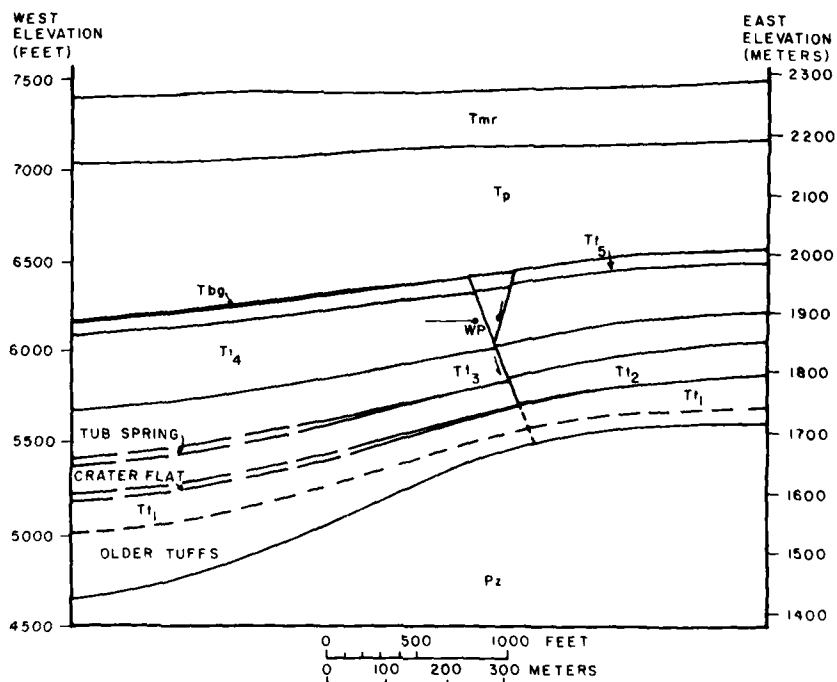
Figure 1b. Approximate west-east cross-section of the Dining Car site.
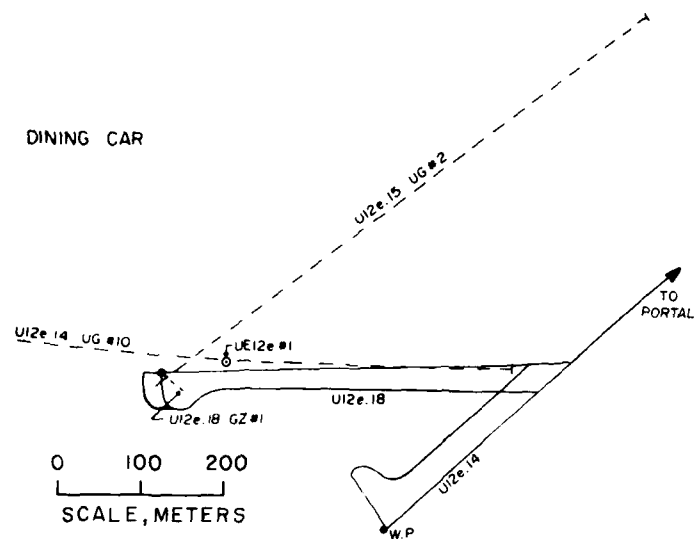
DINING CAR

Figure 2.   Map showing locations of Dining Car drill holes
(plan view).
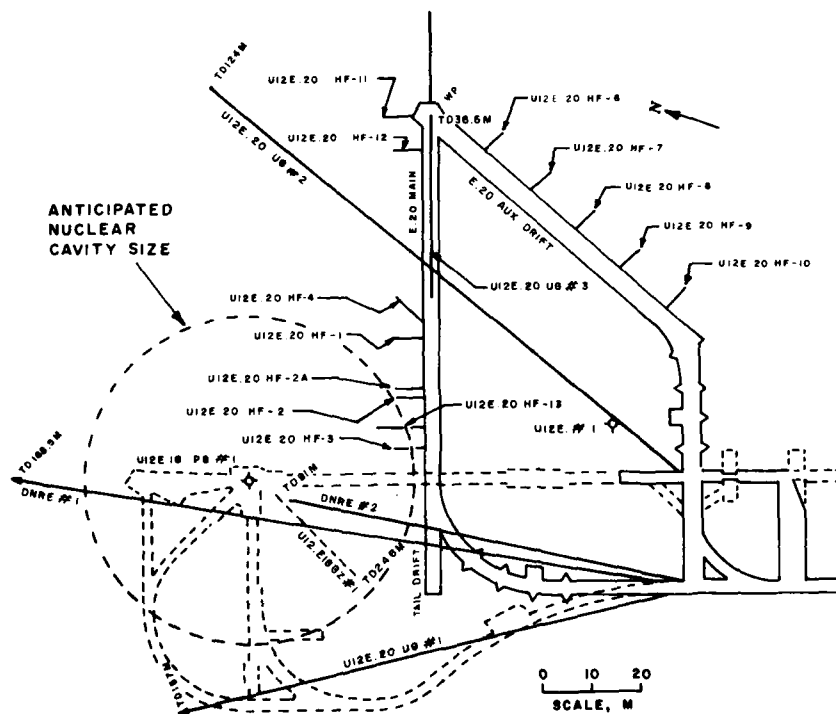
Figure 3.   Drill hole locations (post-Dining Car).
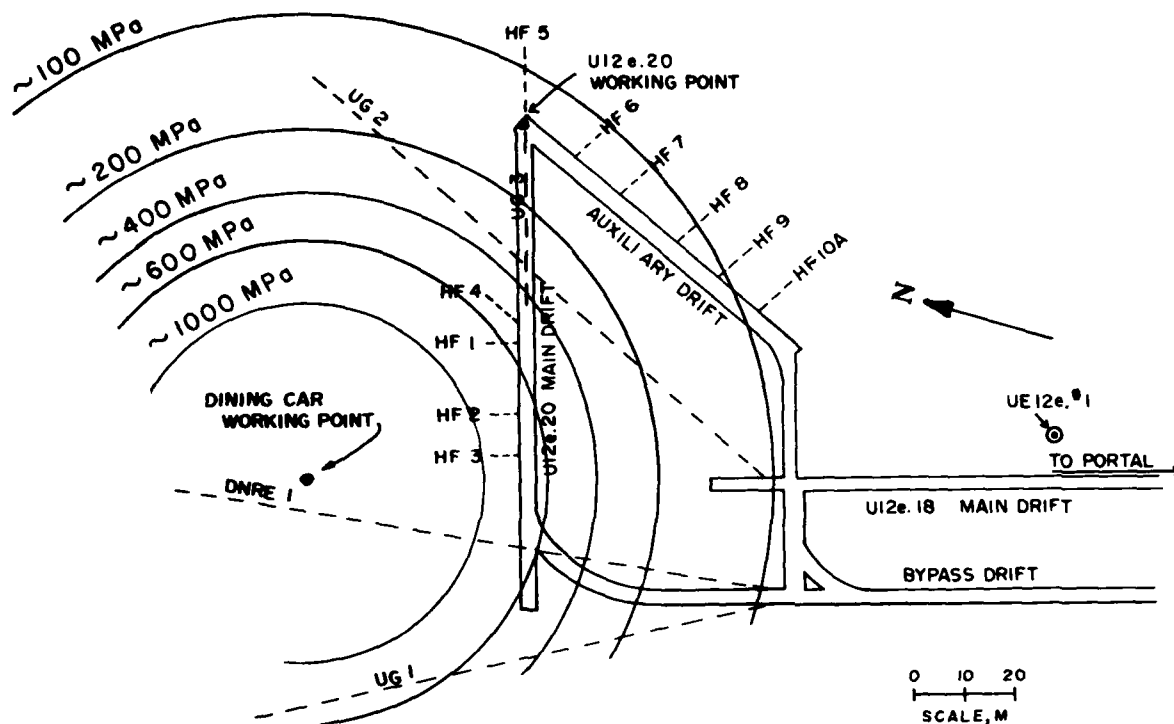
Figure 4. Plan view showing the previous Dining Car location and approximate peak radial stresses, the U12e.20 tunnels, and selected drill holes.

these features were not mapped pre-Dining Car, they are believed to be shock induced.

Mining observations nearest to the Dining Car site (50-60 meters), in a peak stress range of several hundred megapascals, indicate the material to be easily excavated with a tendency to bind together after cutting (i.e. clogging the Alpine Miner). As the mining continued away from the Dining Car site, the rock became more competent and the tendency to slab increased.

SECTION II

PHYSICAL AND MECHANICAL LABORATORY PROPERTIES

The U12e.20 event at the Nevada Test Site required, as for past events, material characterization and hence a material model, for predicting stemming and containment. However, the event configuration was unusual in that the working point and drifts were within 90 meters of a previous event (Dining Car). The U12e.20 material characterization was therefore conducted with consideration given to this unusual condition.

Material properties were determined on core samples taken prior to the Dining Car event from a vertical drill hole located approximately 100 meters southwest of the working point and three drill holes in the horizontal plane of the working point. Post-Dining Car core samples (i.e. U12e.20 samples) were from several drill holes located in the horizontal plane of the U12e.20 main and auxiliary drifts.

Tests were conducted on core samples from the following drill holes:

UE12e#1 (vertical from Mesa top)	
U12e.14 UG#10	
U12e.15 UG#2	Pre-Dining Car (see Figure 2)
U12e.18 GZ#1	
U12e.18 DNRE#1	
U12e.20 UG#1, 2, 3	Post-Dining Car (see Figure 4)
U12e.20 HF#1, 2, 3, 4, 5, 6, 7, 8, 9, 10A	

Material characterization was accomplished by determination of mechanical properties (i.e., a combination of uniaxial strain and triaxial compression tests) and measurement of physical properties and ultrasonic

11

longitudinal and shear wave velocities. Select core samples were also subjected to scanning electron microscopy. The above material properties are summarized in individual tables in the appendix.

Effects of the Dining Car Event: Interest in the effects of nuclear shock loading on tuff material led to comparison of preshot and postshot* Dining Car data. The effects were first observed in a reentry drill hole and in other site investigation holes from which the uniaxial strain tests produced lower stress differences for given confining pressures**. This lower stress difference becomes immediately apparent when preshot and postshot data are plotted together as shown in Figure 5. Uniaxial strain volume change curves also showed a marked difference between preshot and postshot tuffs. When test results are plotted on an expanded scale, postshot tuffs have a significantly larger "foot" than do preshot tuffs, as shown in Figure 6. Strangely enough, however, the postshot tuffs produced lower uniaxial strain permanent volume compactions than did the preshot (the unloading curves are not shown but the data is listed in Tables A1-A7).

It was reasoned that the differences might be explained by the presence of numerous microcracks in the postshot tuff[1], which reopen on unloading. The preshot tuff's permanent volume compactions are primarily due to air filled pore porosity. Thus, the relative small "foot" associated with the usual permanent volume compaction of 1 to 2% by volume. The

---

* The "postshot" data is generally a combination of tuff which was subjected to a peak radial stress of from 100 MPa to 1000 MPa.

** Uniaxial strain tests to 400 MPa confining pressure are conducted to simulate the one-directional stress waves from the nuclear event in addition to providing indicators of material shear strength (i.e. stress-stress response) and gas-filled void content (i.e. stress-strain response).

12
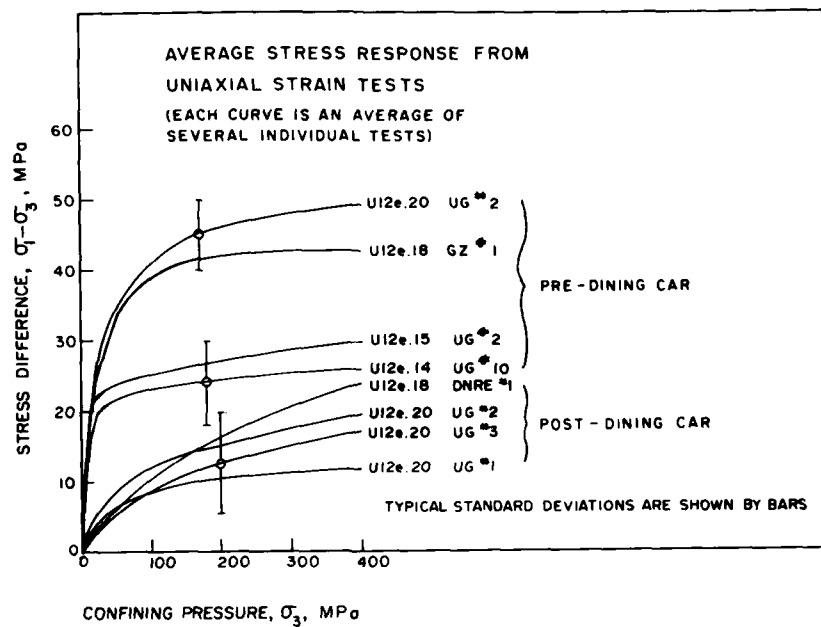
Figure 5. Comparison of preshot and postshot Dining Car uniaxial strain
tests -- stress difference versus confining pressure.
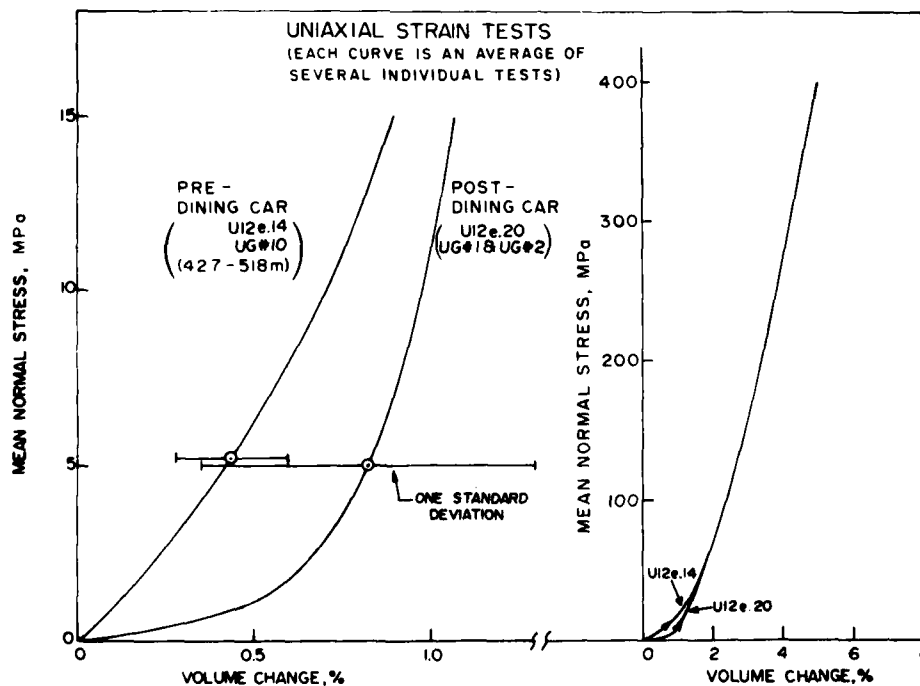
Figure 6. Comparison of preshot and postshot Dining Car uniaxial
strain tests -- mean normal stress versus volume change.

13

apparent air void content of the postshot tuff, on the other hand, is thought to be due to shock-induced microcracks which have been "opened" when relieved of overburden stress and are closed easily at low stresses -- reference the "foot" on the postshot samples. The postshot samples either contain very little, if any, of the original air-filled pore porosity or the existing pores have been filled with water. This latter possibility has been suggested by data on the preshot and postshot Ming Blade tuff[2] and is also reflected in the data contained herein, see Table 1. The bed 4J*numbers represent the average properties of that rock unit through-out the Area 12 tunnel complex. Bed 4J shows identical porosities and moisture contents to that of the pre-Dining Car media (also 4J) but both have noticeably lower porosities and moisture contents than the postshot media.

To address these gas-filled void changes, select postshot samples were hydrostatically loaded to estimated overburden stresses followed by

TABLE 1**

Average Select Properties of Preshot Dining Car
and U12e.20 Media

	Density, gm/cc			Porosity %	Moisture Content %
	As-Received	Dry	Grain		
Dining Car	1.93	1.59	2.44	35	18
(4J)	1.96	1.63	2.47	35	18
Post Dining Car (U12e.20)	1.90	1.51	2.52	40	20.3

* An individual sub-unit within the Tt4 unit shown in Figure 1.
** Compiled by Mr. J. W. LaComb, DNA, Mercury, Nevada.

uniaxial strain loading. It was observed that the foot was virtually eliminated and measured permanent compaction from the uniaxial strain portion of the test was reduced substantially (Tables A6 and A7). Typical tests are shown in Figure 7. This observation suggested that microcracks do apparently close when overburden stresses are applied. Similar tests were conducted on a few preshot tuff samples to determine if the initial hydrostatic compression would eliminate any permanent compaction. The data, however, was not sufficient to draw any conclusions. Further tests comparing preshot and postshot tuff are needed to answer these questions of overburden stress and microcrack effect on material properties.

To investigate microcrack presence, several preshot and postshot tuff samples were subjected to microscopic examination using a scanning electron microscope. Preshot tuff samples were thoroughly examined and
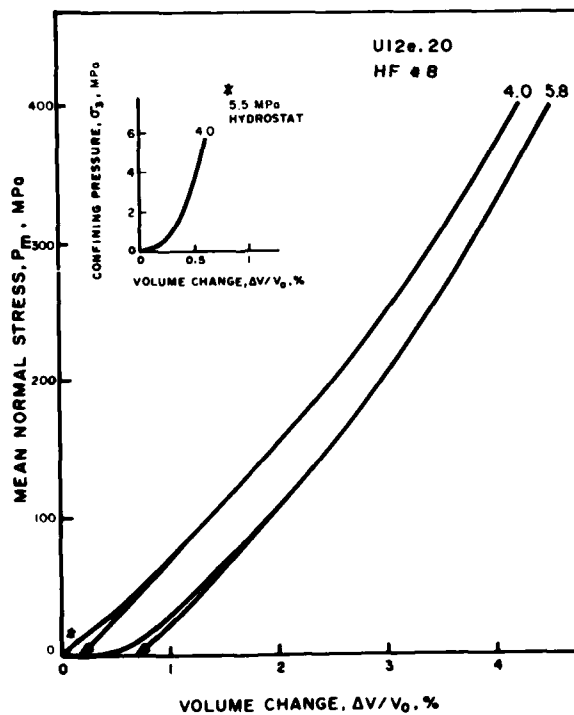
Figure 7. Typical uniaxial strain and hydrostatic compression/uniaxial strain tests on Hybla Gold tuff.

15

few microcracks were observed. Pore structure appeared undamaged and the
zeolite web-like structures often found in the pores were still intact.
Representative preshot photographs are shown in Figure 8. Postshot tuff
samples were examined equally thoroughly and a large number of microcracks
were present in all cases, see Figure 9. The zeolite webbing was partially
broken down in some cases and cleavage planes were occasionally present.
An examination was also made of preshot tuff subjected to a 400 MPa uniaxial
strain test. Figure 10 shows photographs of post uniaxial strain tuff.
There is some indications of damage although not as obvious as in the post-
shot material.

So far, changes in physical properties and the existence of micro-
cracks have been documented. Their effect on the gas-filled void content
has also been discussed and partially verified. The mechanisms behind the
changes in the shear stress response are at this time mostly speculation,
although supportive test data are available.

The lower stress-stress response during the uniaxial strain tests,
Figure 5, could be a result of both the microcracks and the physical pro-
perties changes. Tests have been conducted in which samples were subjected
to two cycles of uniaxial strain loading to roughly simulate fractured
postshot samples[3]. Many of the samples produced a lower stress-stress
curve on the second cycle. There is evidence, therefore, that the exist-
ence of microcracks can lessen the shear stress capacity of the material.
Likewise, a material with high porosity, high moisture content (i.e.
simulating postshot material), and, hence, a lower effective stress,
will also exhibit lower shear stresses.

16
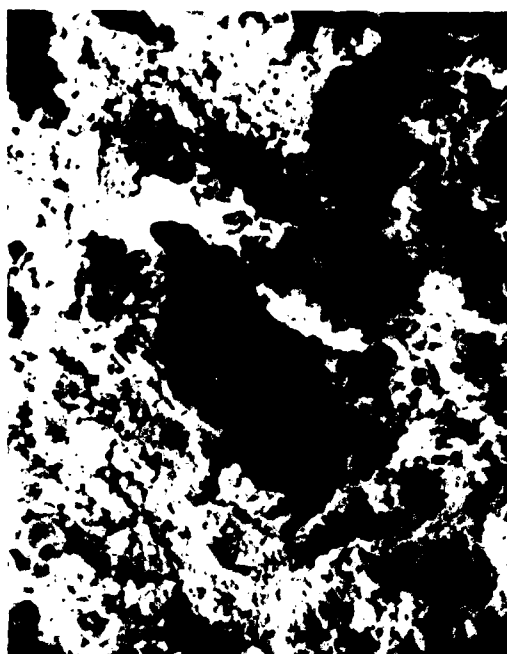
├──────────┤ 50 Microns   ├──────────┤ 50 Microns
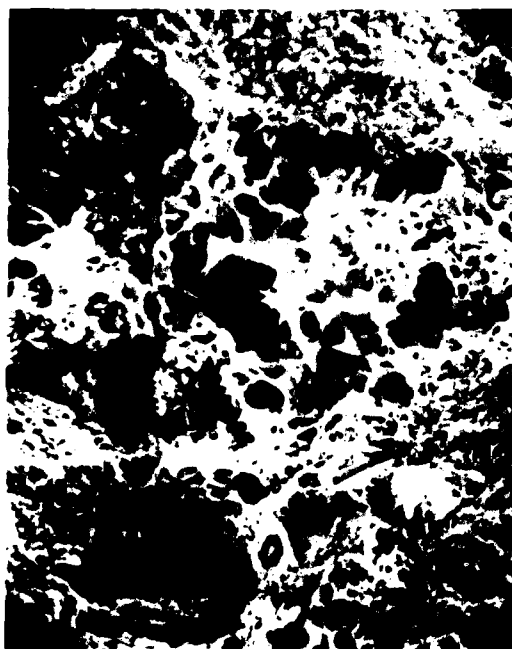
├──────────┤ 50 Microns   ├──────────┤ 25 Microns

Figure 8. ESM photographs of virgin ash-fall tuff from Hybla Gold
           Site.

17
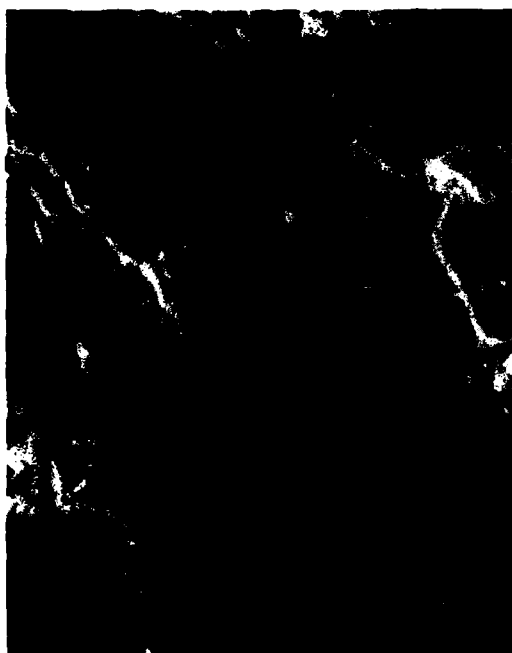
├─────────────┤ 50 Microns   ├─────────────┤ 25 Microns
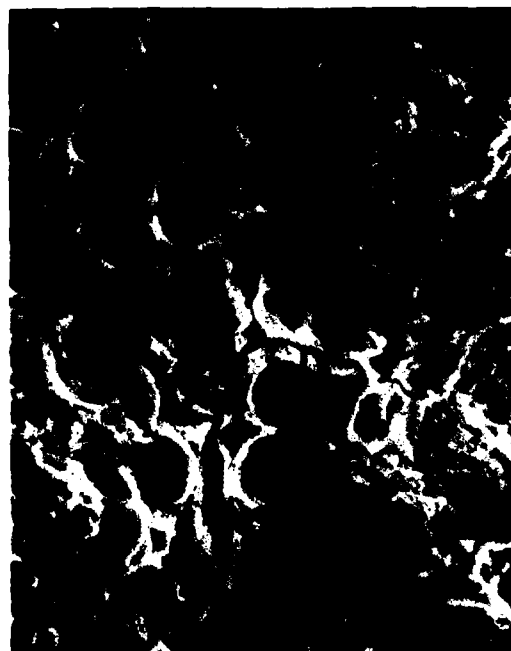
├─────────────┤ 50 Microns   ├─────────────┤ 25 Microns

Figure 9.   ESM photographs of ash-fall tuff subjected to shock wave
from the Dining Car nuclear explosion.

18
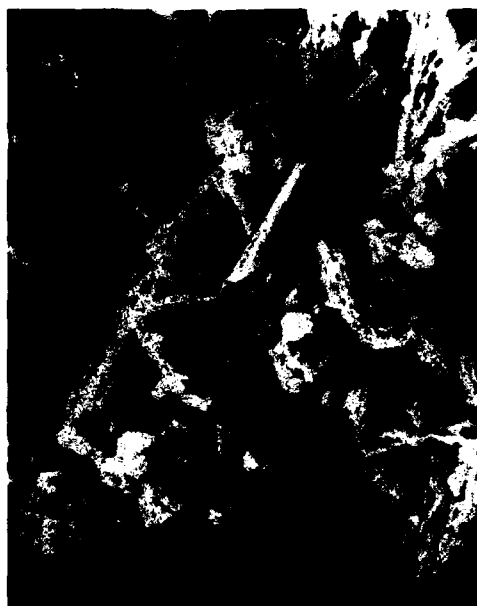
├──────────┤ 12.5 Microns

├──────────┤ 50 Microns
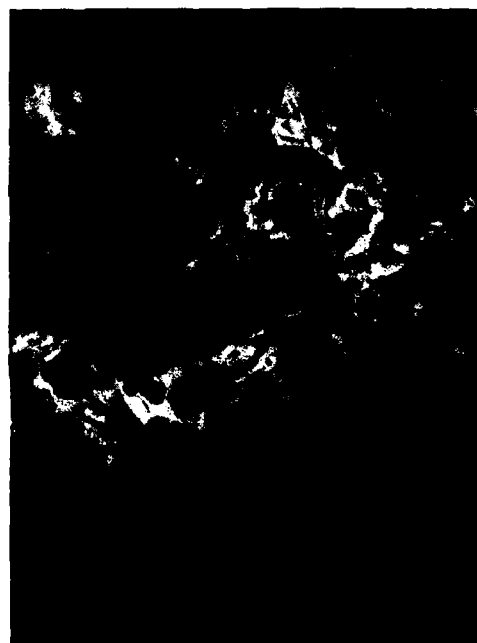
├──────────┤ 25 Microns

├──────────┤ 50 Microns

Figure 10.   ESM photographs of ash-fall tuff subjected to 400 MPa
uniaxial strain test.

19

The ultrasonic p- and s-wave velocities conducted at room conditions
show several regions of low velocities (not seen pre-Dining Car), see
appendix. The decreases were as much as 30 to 50 percent in select areas.
This decrease in ultrasonic velocities could also be a result of both the
microcracks and the physical properties changes. Test results generated at
Terra Tek show ultrasonic longitudinal (p-wave) velocity decreases of up to
25 percent as a result of fracturing by uniaxial compression loading and
direct shearing[4]. With regard to the physical properties changes (primarily
the increase in porosity and moisture content) Figure 11 shows p-wave plotted
versus moisture content for random tunnel bed tuff samples. Although there
is considerable scatter, the data does suggest lower p-wave velocities with
higher water contents.
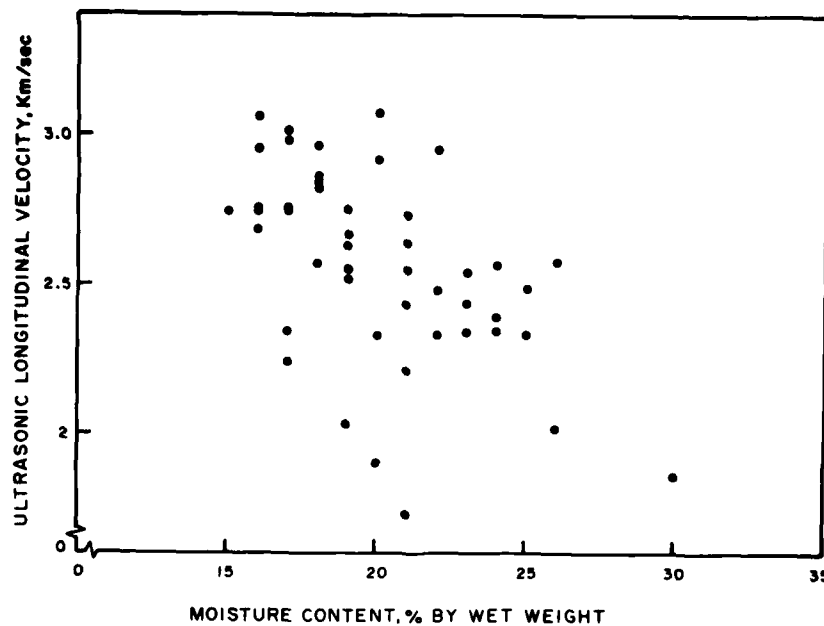
Figure 11. Ultrasonic p-wave velocity versus moisture content
for random Area 12 tunnel bed tuffs.

SECTION III

GEOPHYSICAL PROPERTIES

Seismic velocities were measured for the Dining Car event and they varied from 2400 to 2500 meters per second, which is typical of the bed 4 tuff.

Effects of the Dining Car Event: The seismic velocities measured after the Dining Car event (Figure 12) indicate changes due to the shock loading. Within the "chimney" region (i.e. disjointed) the velocities are, as expected, only about 1500 meters/second (M/S) (the "chimney" region is shown in Figure 3 by the dashed circle around the Dining Car working point). From the "chimney" region out to a radial distance of about 65 meters (i.e. a peak radial stress of about 300 MPa) the velocities ranged from about 2100 M/S to 2200 M/S. The reduction in this region is probably due to the small, tight, discontinuous fractures and faults present as well as possible microfracturing*. As mentioned in the laboratory test program (Section II), the ultrasonic velocities on core samples from this same region substantiated the decrease in velocity.

At a range of 80 to 90 meters (a radial stress of 100 to 200 MPa), the longitudinal seismic velocities were comparable to the pre-Dining Car values. In this same region, however, shear seismic velocities were still noticeably lower than preshot values. A possible explanation is that the microcracks which exist postshot have a more pronounced affect on the shear wave velocity than on the longitudinal wave velocity.

---

* See Section II.

21
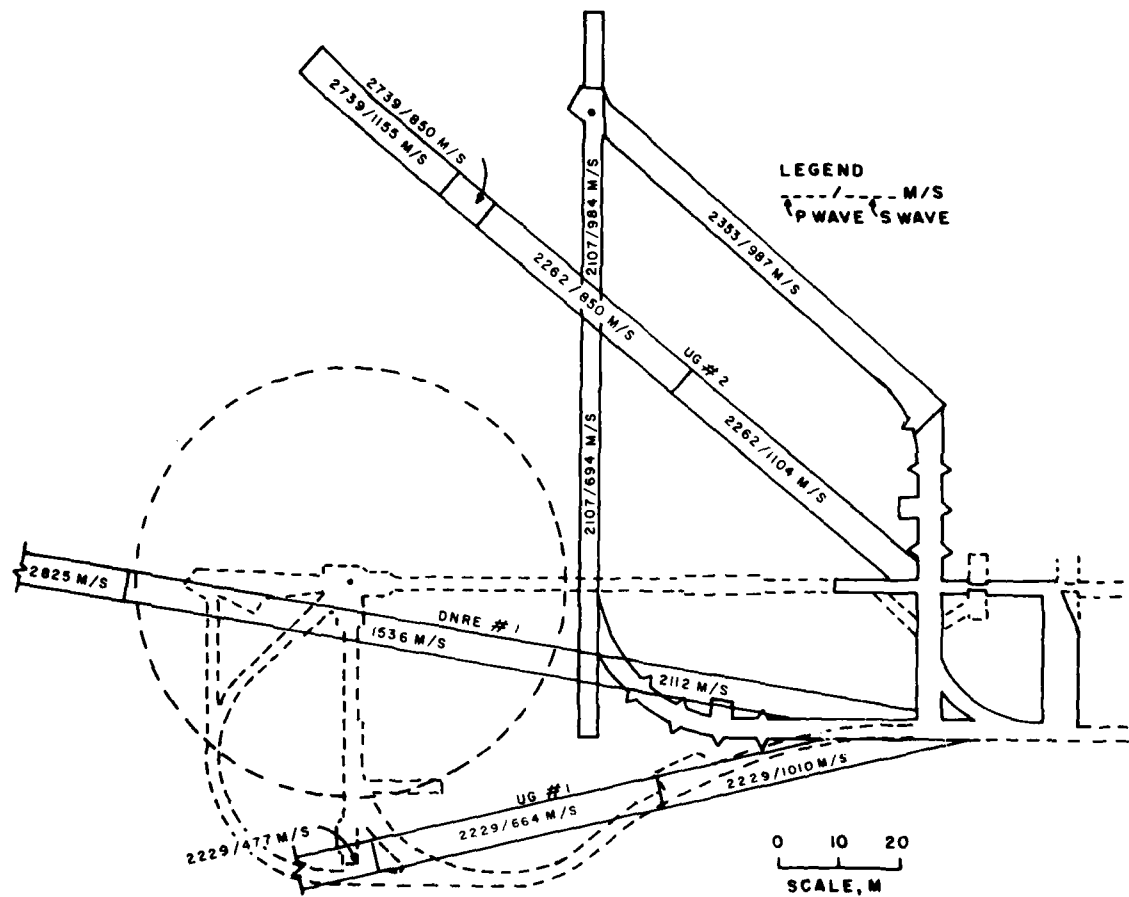
Figure 12. Plan view of the U12e.20 complex showing longitudinal and shear wave velocities.

22

SECTION IV

GEOMECHANICAL PROPERTIES

Since the *in situ* stress is an important parameter in determining
the potential for a particular site to contain a nuclear event, con-
siderable effort was spent in obtaining the stresses, via the overcore
technique and hydraulic fracturing. The Dining Car region indicated,
via hydraulic fracturing, a minimum *in situ* stress of about 3.8 MPa
and via the overcore technique, approximately 2.8 MPa.

Results of the overcore data are preliminary since the technique
requires use of a Young's modulus and there are uncertainties in inte-
grating the laboratory measured moduli with the overcore data.

Minimum *in situ* stress via overcoring in another "e" tunnel loca-
tion (several hundred meters south of the U12e.20 site) was about 3.4
MPa. An average or typical value for minimum *in situ* stress in the
subject area would be between 3.0 and 3.5 MPa.

Effects of the Dining Car Event: In anticipation of the U12e.20
event (i.e. post-Dining Car), over forty hydraulic fracture tests and
several overcore experiments were performed. Figure 13 shows the apparent
minimum *in situ* stresses as a function of distance from the Dining Car
event and peak radial stress. Near the Dining Car chimney, stresses had
decreased to about 1.2 MPa. There appears to be "higher than normal"
stresses near the U12e.20 location but further data are necessary to
address this phenomena. The results indicate that the Dining Car stress
wave did not have an apparent affect on the *in situ* stress field (at least

23

minimum) at a peak stress less than about 100 MPa (i.e. a range of about

85 meters). However, affects are apparent as the peak stress increases

to 1000-2000 MPa.
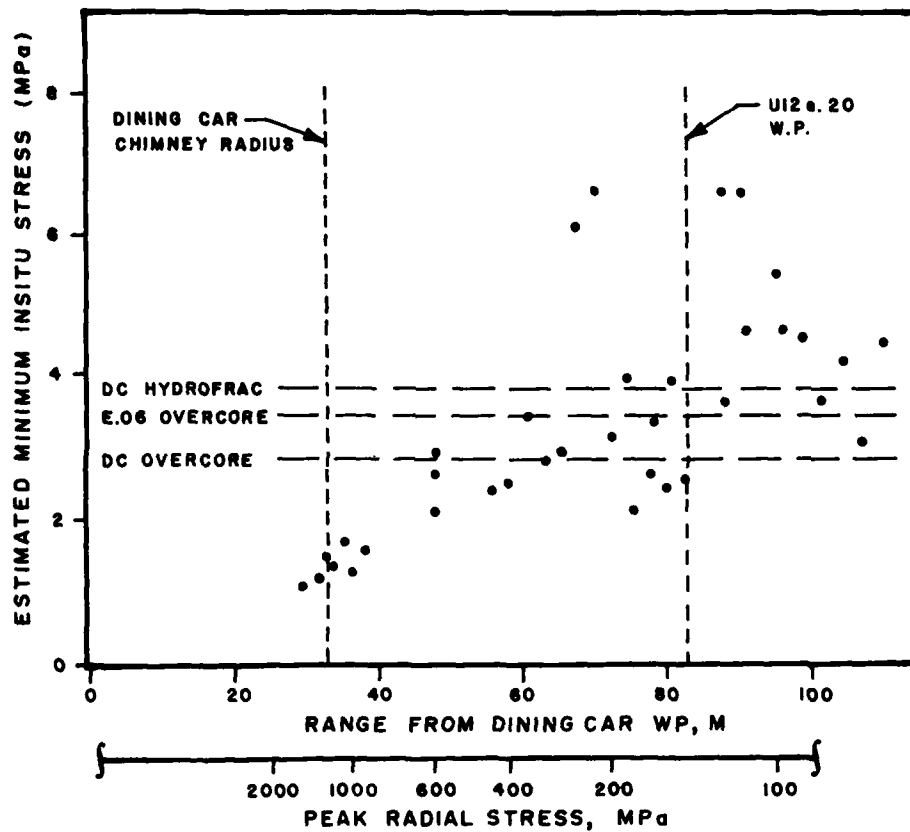
Figure 13. Minimum *in situ* stresses as a function of distance
from the Dining Car event and peak radial stresses.

CONCLUSIONS

The Dining Car event provided an opportunity to study the changes
in rock material (tuff) subjected to shock waves. In this case, the
range of peak radial stress was from 1000 to 100 MPa.

Geology: There was no evidence of bedding plane shifts or fault
movement. There were, however, few faults mapped pre-Dining Car. The
post-Dining Car media does contain small, tight and discontinuous frac-
tures and faults, some of which showed evidence of horizontal movement.
These features are believed to be shock induced.

The ease of excavation in the tuff which had been subjected to a
stress of several hundred megapascals (i.e. 500-700 MPa), as compared
to preshot mining, suggests changes such as a decrease in the shear
strength of the material.

Material Properties: Of significance were:

1) changes in the characteristics of volume strain and permanent
    volume compaction during uniaxial strain tests,

2) an apparent decrease in the shear stress capacity during uni-
    axial strain loading, and

3) a decrease in the ultrasonic p- and s-wave velocities.

Further examination produced evidence that densities, porosities, and
moisture contents had increased, suggesting fluid migration into exist-
ing or induced cracks and pores. Also, subsequent electron scanning
microscope pictures showed numerous microcracks in the postshot material.

The mechanical properties changes (numbers 1 through 3 above)
appear to be explainable via the changes in the physical characteristics.

25

In most cases, data are presented to verify the proposed relationships between the changes.

Geophysics: The seismic velocities decreased from the pre-Dining Car values (2500-2600 M/S) to about 1500 M/S through the Dining Car "chimney". The tuff which had been subjected to several hundred mega-pascals peak stress (~400 to 800 MPa) showed a decrease of 10 to 20 percent -- from 2500 M/S to ~2100 M/S. Outside of a stress of about 200 MPa, there was little apparent change in the longitudinal seismic velocities. The shear wave velocities, however, were affected more noticeably even beyond the 100 MPa stress level.

Geomechanics: There were no apparent changes in the *in situ* stress field outside of about 100 MPa peak radial stress. As the peak stresses increased to 1000 MPa, however, the apparent minimum *in situ* stress decreased to about 1.2 MPa, as compared to a pre-Dining Car stress of 3-3.5 MPa. These measurements were obtained via a combination of hydraulic fracturing and overcoring.

In summary, the *in situ* stress state and material properties were affected noticeably when subjected to peak radial stresses greater than 100 MPa. There are likely some changes at lower stresses but their magnitudes were not quantified for this application.

26

REFERENCES

1. Mr. J. W. LaComb, Defense Nuclear Agency Field Command, Mercury, Nevada, Personal Communication, July 1977.

2. Butters, S. W., C. N. Snow, and A. H. Jones, "Nevada Test Site 'Two-In-One Concept' Evaluation: Comparison of Preshot and Post-shot Material Properties," Terra Tek Report TR 76-61, August 1976.

3. Gardiner, D. S., and S. W. Butters, "Material Properties for Diablo Hawk Event," Terra Tek Report TR 77-43, June 1977.

4. Lingle, R., R. S. Rosso, and L. M. Buchholdt, "An Investigation to Determine the Effect of Fracture on the Ultrasonic Velocities in Ash-Fall Tuff," Terra Tek Report TR 75-20, DNA Contract No. 001-75-C-0260, May 1975.

APPENDIX

PRE-DINING CAR DATA

UE12e#1
U12e.14 UG#10
U12e.15 UG#2
U12e.18 GZ#1

TABLE A1

Physical Properties, Uniaxial Strain Measured Permanent Compaction, and
Ultrasonic Longitudinal and Shear Wave Velocities of
UE12e#1 Tuffs

DRILL HOLE FOOTAGE (M)	DENSITY (gm/cc)			WATER BY WET WEIGHT (%)	POROSITY (%)	SATURATION (%)	CALC. AIR VOIDS (%)	MEAS. PERMANENT COMP. (%)	VELOCITY (km/sec)	
	AS-RECEIVED	DRY	GRAIN						LONG	SHEAR
UE12e.#1	Meas.	Cal.	Meas.	Meas.	Cal.	Cal.	Cal.	Meas.	Meas.	Meas.
345.6	1.80	1.38	2.42	23	43	97	0.9	1.8	2.50	1.23
349.3	1.85	1.54	2.42	17	36	86	5.5	2.0	2.99	1.69
353.0	1.84	1.47	2.42	20	39	94	2.3	3.1	2.46	1.28
357.2	1.79	1.41	2.42	21	42	90	3.7	1.0	2.44	1.25
360.3	1.88	1.53	2.47	18	38	90	2.9	3.0	2.66	1.37
364.2	2.06	1.83	2.44	11	25	91	1.9	1.1	3.08	1.47
368.5	1.94	1.59	2.45	18	35	99	0.1	0.7	3.15	1.62
371.9	1.94	1.61	2.45	17	34	96	1.3	1.3	2.93	1.50
376.1	1.88	1.51	2.47	20	39	96	1.9	1.5	2.57	1.24
379.8	1.88	1.55	2.37	18	34	97	1.6	2.1	2.89	1.58
383.7	1.80	1.46	2.44	19	40	85	6.2	3.2	2.62	1.05
387.4	1.93	1.56	2.58	19	39	93	2.5	1.7	2.47	1.09
391.4	1.94	1.59	2.53	18	37	94	2.1	1.7	3.01	1.40
395.0	1.99	1.65	2.58	17	36	94	2.0	2.7	2.50	1.11
398.7	1.82	1.44	2.42	21	40	94	2.5	2.2	2.67	1.51
402.3	1.81	1.41	2.43	22	42	95	2.0	3.4	2.54	1.18
406.3	1.85	1.46	2.44	21	40	97	1.2	1.4	2.75	1.43
410.0	1.80	1.42	2.43	21	41	91	3.6	2.3	2.41	1.18
413.9	1.81	1.45	2.47	20	41	87	5.3	3.1	2.17	1.03
417.9	1.85	1.46	2.49	21	42	94	2.4	2.4	2.18	1.10
421.8	1.81	1.42	2.45	22	42	94	1.6	1.0	2.48	1.06

29

PRECEDING PAGE BLANK-NOT FILLED

TABLE A2

Physical Properties, Uniaxial Strain Measured Permanent Compaction, and
Ultrasonic Longitudinal and Shear Wave Velocities of
U12e.14 UG#10 Tuffs

DRILL HOLE FOOTAGE (M)	DENSITY (gm/cc)			WATER BY WET WEIGHT (%)	POROSITY (%)	SATURATION (%)	CALC. AIR VOIDS (%)	MEAS. PERMANENT COMP. (%)	VELOCITY (km/sec)	
	AS-RECEIVED	DRY	GRAIN						LONG	SHEAR
U12e.14 UG#10	Meas.	Cal.	Meas.	Meas.	Cal.	Cal.	Cal.	Meas.	Meas.	Meas.
198.1	1.89	1.47	2.43	22	39	~100	~0	0.4	2.95	1.47
212.8	1.87	1.51	2.44	19	38	94	2.1	1.3	2.67	1.32
227.7	2.07	1.71	2.55	17	33	~100	~0	0.6	2.76	1.41
243.2	1.97	1.59	2.51	19	36	~100	~0	1.4	2.52	1.07
258.5	1.83	1.40	2.42	23	42	~100	~0	1.0	2.44	1.12
274.6	1.94	1.61	2.49	17	35	93	2.3	0.9	3.01	1.31
289.9	1.93	1.56	2.45	19	36	~100	~0	1.4	2.75	1.36
306.6	2.00	1.64	2.42	18	32	~100	~0	1.3	2.84	1.40
320.3	1.92	1.57	2.32	18	32	~100	~0	0.8	2.96	1.61
325.2								2.4		
327.4	1.83	1.41	2.38	23	41	~100	~0	4.4	2.45	1.06
329.2								2.2		
335.0	1.90	1.54	2.42	19	36	99	0.3	1.1	2.63	1.15
342.9	2.05	1.81	2.40	12	25	99	0.7	0.9	3.67	2.14
350.5	1.93	1.58	2.42	18	35	~100	~0	1.1	2.86	1.70
358.8	1.84	1.49	2.46	19	39	89	4.4	1.5	2.57	1.15
365.2	1.81	1.37	2.42	24	43	~100	~0	2.5	2.34	1.01
372.8	1.90	1.50	2.45	21	39	~100	~0	1.0	2.55	1.20
381.0	1.85	1.44	2.49	22	42	97	1.2	1.2	2.33	0.84
388.3	1.88	1.52	2.52	19	40	90	3.7	0.8	2.55	1.19
395.9	1.85	1.44	2.47	22	42	98	0.7	1.3	2.34	1.01
403.3	1.86	1.46	2.48	21	41	96	1.0	1.9	2.43	1.12
405.7	1.77	1.35	2.43	24	45	96	2.0	1.2	2.39	0.99
412.7	1.98	1.65	2.50	17	34	99	0.4	0.8	2.75	1.36
420.3	1.91	1.57	2.42	18	35	97	1.0	1.1	2.65	1.13
427.9	2.01	1.68	2.49	16	32	99	0.3	0.6	2.76	1.31
435.0	2.00	1.68	2.58	16	34	95	1.7	1.3	3.06	1.36
443.2	2.02	1.70	2.51	16	32	99	0.3	1.2	2.95	1.36
446.5	2.01	1.65	2.51	18	34	~100	~0	1.5		
450.8	1.91	1.60	2.46	16	35	87	4.4	2.9	2.74	1.36
455.1	2.05	1.72	2.54	16	32	~100	~0	1.1		
458.4	2.00	1.68	2.50	16	33	98	0.8	0.9	2.68	1.18
465.7	1.94	1.59	2.49	18	36	97	1.0	1.1	2.69	1.25
474.3	1.77	1.33	2.45	25	46	97	1.4	1.8	2.33	1.03
482.0	1.83	1.44	2.41	21	40	97	1.3	2.7	2.73	1.26
489.2	1.81	1.39	2.48	23	44	95	2.2	1.9	2.54	1.12
496.5	1.89	1.53	2.39	19	36	100	0.1	1.0		
501.4	1.96	1.64	2.43	16	33	99	0.4	0.9		
508.1	1.87	1.54	2.38	18	35	95	1.7	0.7	2.82	1.37
517.6	1.89	1.53	2.45	19	37	96	1.4	1.3	2.52	1.17

TABLE A3

Physical Properties, Uniaxial Strain Measured Permanent Compaction, and
Ultrasonic Longitudinal and Shear Wave Velocities of
U12e.15 UG#2 Tuffs

DRILL HOLE FOOTAGE (M)	DENSITY (gm/cc)			WATER BY WET WEIGHT (%)	POROSITY (%)	SATURATION (%)	CALC. AIR VOIDS (%)	MEAS. PERMANENT COMP. (%)	VELOCITY (km/sec)	
	AS-RECEIVED	DRY	GRAIN						LONG	SHEAR
U12e.15 UG#2	Meas.	Cal.	Meas.	Meas.	Cal.	Cal.	Cal.	Meas.	Meas.	Meas.
631.9	1.93	1.53		21				1.6		
647.4	2.01	1.67		17				1.2		
663.6	1.91	1.55		19				1.0		
677.9	2.02	1.73		14				0.6		
693.1	1.80	1.37		24				1.8		
708.1	1.90	1.53		19				2.0		
723.6	1.91	1.52		20				0.9		
737.3	1.96	1.63	2.48	17	34	97	1.3	1.9		
751.3	2.01	1.69	2.50	16	32	99	0.4	1.5		
755.3	1.99	1.69	2.43	15	30	98	0.5	2.2		

TABLE A4

Physical Properties, Uniaxial Strain Measured Permanent Compaction, and
Ultrasonic Longitudinal and Shear Wave Velocities of
U12e.18 GZ#1 Tuffs

DRILL HOLE FOOTAGE (M)	DENSITY (gm/cc)			WATER BY WET WEIGHT (%)	POROSITY (%)	SATURATION (%)	CALC. AIR VOIDS (%)	MEAS. PERMANENT COMP. (%)	VELOCITY (km/sec)	
	AS-RECEIVED	DRY	GRAIN						LONG	SHEAR
U12e.18 GZ#1	Meas.	Cal.	Meas.	Meas.	Cal.	Cal.	Cal.	Meas.	Meas.	Meas.
2.7	2.02	1.72	2.50	15	31	97	1.1	0.7	3.30	1.80
7.3	1.85	1.44	2.47	22	42	99	0.5	1.7	2.64	1.23
8.8	1.85	1.44	2.44	22	41	99	0.4	3.9	2.63	1.25
10.7	1.84	1.43	2.48	23	42	98	1.0	3.0		
14.6	2.00	1.72	2.44	14	30	94	1.8	0.6	3.36	1.87
18.6	1.84	1.46	2.49	21	41	92	3.3	1.2	2.64	1.30
21.3	1.84	1.45	2.45	22	41	97	1.4	2.3	2.57	1.30
21.9	1.81	1.37	2.47	25	45	99	0.3	2.1	2.49	1.08
24.7	1.87	1.52	2.46	19	38	92	3.2	2.1	3.46	1.75

POST-DINING CAR DATA

U12e.18 DNRE#1
U12e.20 UG#1, 2, 3
U12e.20 HF#1-10A

TABLE A5

Physical Properties, Uniaxial Strain Measured Permanent Compaction, and
Ultrasonic Longitudinal and Shear Wave Velocities of
U12e.18 DNRE#1 Tuff

DRILL HOLE FOOTAGE (M)	DENSITY (gm/cc)			WATER BY WET WEIGHT (%)	POROSITY (%)	SATURATION (%)	CALC. AIR VOIDS (%)	MEAS. PERMANENT COMP. (%)	VELOCITY (km/sec)	
	AS-RECEIVED	DRY	GRAIN						LONG	SHEAR
U12e.18 DNRE#1	Meas.	Cal.	Meas.	Meas.	Cal.	Cal.	Cal.	Meas.	Meas.	Meas.
12.2	1.97	1.64	2.52	16.7	34.9	94.3	2.0	1.0	2.72	1.29
21.0	1.80	1.40	2.49	22.5	44.0	92.1	3.5	2.4	2.24	1.13
24.7	1.87	1.49	2.44	20.1	38.9	96.7	1.3	0.8	2.38	1.19
30.8	1.89	1.53	2.51	19.2	39.2	92.7	2.9	1.1	2.67	1.41
37.2	1.89	1.52	2.50	19.6	39.3	94.2	2.3	1.0	2.11	1.43
44.5	1.79	1.40	2.47	22.0	43.5	90.6	4.1	2.7	1.70	--
51.5	1.77	1.33	2.47	24.6	46.0	94.7	2.4	1.2	--	--

TABLE A6

Physical Properties, Uniaxial Strain Measured Permanent Compaction, and Ultrasonic Longitudinal and Shear Wave Velocities of U12e.20 UG#1,2,&3 Tuffs

DRILL HOLE FOOTAGE (M)	DENSITY (gm/cc)			WATER BY WET WEIGHT (%)	POROSITY (%)	SATURATION (%)	CALC. AIR VOIDS (%)	MEAS.** PERMANENT COMP. (%)	VELOCITY (km/sec)	
	AS-RECEIVED	DRY	GRAIN						LONG	SHEAR
U12e.20 UG#1	Meas.	Cal.	Meas.	Meas.	Cal.	Cal.	Cal.	Meas.	Meas.	Meas.
10.7	1.89	1.56	2.53	18.1	38.5	89.3	4.1	0.9	2.24	0.95
20.7	2.08	1.82	2.47	12.3	26.0	98.3	0.4	0.5	3.37	1.82
27.7 m.s.*	1.98	1.65	2.54	16.8	35.0	94.9	1.8	---	--	--
29.9	1.77	1.29	2.63	27.1	50.9	94.3	2.9	1.7	2.42	1.20
35.1	1.78	1.32	2.66	26.1	50.5	91.8	4.1	1.9	2.44	1.40
12.4	1.74	1.31	2.53	24.6	48.0	88.9	5.3	1.9	1.91	0.93
48.8 m.s.*	1.80	1.38	2.49	23.3	44.5	94.2	2.6	---	--	--
57.0 m.s.*	1.74	1.30	2.51	25.4	48.3	91.5	4.1	---	--	--
61.3	1.83	1.42	2.54	22.6	44.2	93.7	2.8	0.1	1.91	0.73
69.5	1.94	1.60	2.48	17.7	35.6	96.4	1.3	1.1	2.28	1.24
U12e.20 UG#2										
6.4	1.95	1.62	2.48	17.0	34.7	95.5	1.6	---	3.18	1.87
14.0	1.89	1.56	2.46	17.4	36.5	90.0	3.7	1.0	2.44	1.18
21.0	1.95	1.59	2.49	18.3	36.0	99.1	0.3	0.4	2.87	1.39
29.9	1.98	1.66	2.51	16.2	33.9	94.8	1.8	0.4	2.98	1.40
37.5	1.82	1.38	2.50	24.0	44.6	97.7	1.1	0.6	2.35	0.99
45.7	1.88	1.48	2.50	21.1	40.6	97.4	1.0	1.1	2.25	1.15
53.0	1.89	1.48	2.53	21.8	41.6	99.0	0.4	0.3	2.47	1.37
61.0	1.92	1.53	2.52	20.1	39.2	98.8	0.5	0.6	2.08	1.13
68.6	1.91	1.50	2.55	21.6	41.3	100.0	0	0.4	2.21	1.20
75.9	1.88	1.49	2.50	20.9	40.5	96.9	1.3	0.7	2.19	1.10
82.9	1.99	1.65	2.60	16.9	36.4	92.3	2.8	0.7	2.43	1.12
91.4	1.92	1.55	2.53	19.4	38.8	95.8	1.6	1.2	2.29	1.15
106.7	1.88	1.49	2.49	20.6	40.1	96.8	1.3	1.6	2.43	1.40
114.0	1.95	1.57	2.55	19.4	38.4	98.7	0.5	0.3	2.30	1.12
121.3	1.88	1.48	2.47	21.0	39.9	99.0	0.4	0.2	2.51	1.30
U12e.20 UG#3								HYD/1-D		
0.6	1.92	1.55	2.56	19.1	39.3	93.2	2.6	0.8	2.62	1.36
1.5	1.93	1.55	2.57	19.6	39.6	95.4	1.8	0.8/0.2	2.39	1.27
3.4	1.89	1.50	2.54	20.4	40.8	94.6	2.2	0.1	2.22	1.49
5.5	1.86	1.45	2.56	22.0	43.3	94.4	2.4	0.6/0.1	2.32	1.30
7.3	1.88	1.49	2.55	20.8	41.6	94.0	2.5	0.7	2.30	1.52
9.1	1.89	1.49	2.53	21.2	41.1	97.4	1.1	0.4/0.8	2.04	1.16
10.7	1.93	1.56	2.54	19.1	38.6	95.7	1.7	0.5	2.30	1.48
11.9	1.93	1.55	2.55	19.6	39.1	96.6	1.3	0.3/0.3	2.26	1.35
13.1	1.91	1.52	2.51	20.5	39.5	99.1	0.3	0.2	2.50	1.37
14.9	1.93	1.57	2.56	18.8	38.8	93.6	2.5	1.3/0.2	2.22	1.34
16.5	1.90	1.52	2.52	20.2	39.9	96.3	1.4	0.1	2.82	1.21
18.3	1.98	1.62	2.57	18.3	37.1	97.8	0.8	0.5/0.2	2.53	1.51
19.5	1.95	1.58	2.49	18.8	36.4	100.0	0	1.8	3.07	1.49
21.0	1.93	1.56	2.54	19.4	38.8	96.6	1.3	0.7/<0.1	2.33	1.48
22.6	1.95	1.59	2.49	18.6	36.2	100.0	0	0.5	2.51	1.46
24.1	1.93	1.56	2.53	19.3	38.4	96.9	1.2	0.8/<0.1	2.65	1.54
25.6	1.88	1.48	2.51	21.2	41.0	97.3	1.1	0.3	2.86	1.29
27.1	1.85	1.45	2.52	21.4	42.3	93.6	2.7	1.3/<0.1	2.53	1.38
29.0	1.89	1.51	2.46	20.2	38.7	98.7	0.5	0.5	2.53	1.41
30.2	1.89	1.52	2.56	19.8	40.8	91.7	3.4	0.9/<0.1	2.31	1.27
32.3	1.91	1.55	2.48	19.1	37.7	96.8	1.2	0.6	2.51	1.28
33.2	1.73	1.27	2.42	26.8	47.7	97.3	1.3	0.7/<0.1	2.19	1.27
34.4	1.74	1.30	2.42	25.5	46.3	95.8	2.3	0.6	2.67	1.36
36.0	1.95	1.59	2.48	18.5	35.9	100.0	0	0.7	2.91	1.46
36.9	1.94	1.59	2.57	17.8	38.1	90.6	3.1	0.4/<0.1	2.39	1.43

* Moisture sample (i.e. the amount or condition of material limited the test program to measurement of only "physical properties").

** The double figures in the "measured permanent compaction" column reflect the volume compactions resulting from hydrostatic compression followed by uniaxial strain loading. See Section II for further details.

33

TABLE A7

Physical Properties, Uniaxial Strain Measured Permanent Compaction, and Ultrasonic Longitudinal and Shear Wave Velocities of U12e.20 HF#1-10A Tuffs

DRILL HOLE FOOTAGE (M)	DENSITY (gm/cc)			WATER BY WET WEIGHT (%)	POROSITY (%)	SATURATION (%)	CALC. AIR VOIDS (%)	MEAS. PERMANENT COMP. (%)	VELOCITY (km/sec)	
	AS-RECEIVED	DRY	GRAIN						LONG	SHEAR
U12e.20 HF#1	Meas.	Cal.	Meas.	Meas.	Cal.	Cal.	Cal.	Meas.	Meas.	Meas.
1.8	1.89	1.50	2.52	20.7	40.5	96.5	1.4	0.9/-0.1	2.14	1.26
4.9	1.88	1.49	2.50	20.5	40.2	95.8	1.7	M.S.	M.S.	M.S.
U12e.20 HF#2										
3.0	1.80	1.39	2.47 *	3.0	43.7	94.7	2.7	0.8/<0.1	1.93	1.07
U12e.20 HF#3										
1.5	1.79	1.35	2.49	24.6	45.8	96.1	1.8	0.3/0.4	1.80	1.20
U12e.20 HF#4										
0.3	1.94	1.57	2.55	19.1	38.4	96.4	1.4	0.8/0.4	2.16	1.26
2.7	1.96	1.60	2.55	18.4	37.3	96.7	1.4	0.9/<0.1	1.98	1.12
6.4	1.87	1.45	2.49	22.4	41.7	100.0	0	0.5	2.13	1.12
7.6	1.89	1.49	2.52	20.9	40.7	97.1	1.2	0.7	1.76	0.82
U12e.20 HF#5										
0.3	1.94	1.59	2.54	17.9	37.3	93.2	2.6	0.6	2.50	1.33
1.5	1.93	1.57	2.49	18.5	36.8	96.8	1.2	0.7/<0.1	2.48	1.33
2.7	1.90	1.52	2.50	19.8	39.0	96.3	1.4	0.5	2.42	1.35
4.6	1.90	1.52	2.50	20.1	39.3	97.3	1.1	0.8/<0.1	2.57	1.36
6.7	1.92	1.54	2.51	19.6	38.5	97.8	0.8	1.2	2.72	1.45
8.5	1.92	1.56	2.51	18.6	37.7	94.7	2.0	0.7/0.6	2.73	1.36
9.8	1.79	1.39	2.44	22.4	43.1	93.1	3.0	1.1	2.62	1.50
11.3	1.74	1.31	2.46	24.9	46.8	92.6	3.5	1.0/<0.1	2.18	1.23
12.5	1.97	1.63	2.48	17.3	34.4	99.4	0.2	0.5	2.83	1.59
13.4	1.92	1.54	2.46	19.6	37.3	100.0	0	0.6/<0.1	2.57	1.38
14.9	2.03	1.71	2.55	15.9	33.1	97.7	0.8	0.4	2.60	1.17
16.8	1.99	1.67	2.46	16.2	32.2	100.0	0	0.3/-0.1	2.56	1.19
18.0	2.06	1.75	2.57	15.2	32.0	97.8	0.7	0.4	2.66	1.19
20.1	2.03	1.71	2.60	16.0	34.4	94.4	1.9	0.7/0.1	2.31	1.04
21.0	1.99	1.66	2.54	16.5	34.6	94.9	1.7	0.7	2.23	1.05
U12e.20 HF#6										
1.8	1.82	1.40	2.49	22.9	43.7	95.5	2.0	0.8/0	2.06	1.10
4.9	1.87	1.51	2.46	19.4	38.7	93.7	2.4	0.4	2.12	1.41
U12e.20 HF#7										
1.2	1.94	1.59	2.53	18.3	38.0	93.8	1.4	0.4/0	2.52	1.50
3.4	1.87	1.48	2.49	20.9	40.6	96.1	1.6	0.7	2.98	1.41
5.2	1.91	1.55	2.52	19.0	38.6	93.9	2.4	0.5/0	2.03	1.34
U12e.20 HF#8										
1.5	1.96	1.62	2.42	17.2	32.9	100.0	0	1.0	2.69	1.70
4.0	1.95	1.59	2.57	18.5	38.2	94.7	2.0	0.7/0.2	2.24	1.78
5.8	1.96	1.60	2.54	18.2	36.9	96.9	1.2	0.7	2.59	1.14
U12e.20 HF#9										
1.2	1.85	1.44	2.52	22.3	43.0	96.0	1.8	0.7/0.5	2.35	1.47
3.4	1.85	1.44	2.50	22.4	42.6	97.3	1.1	0.9	2.42	1.35
5.5	1.87	1.46	2.55	21.6	42.5	95.1	2.1	1.1/0.1	2.61	1.25
U12e.20 HF#10a										
1.8	2.00	1.67	2.46	16.3	32.0	100.0	0	0.5	3.06	1.75
4.0	1.94	1.56	2.52	19.4	37.9	99.0	0.4	0.9/0.4	2.31	1.40
6.1	1.89	1.53	2.45	18.9	37.4	95.4	1.7	1.5	2.73	1.58

DISTRIBUTION LIST

DEPARTMENT OF DEFENSE

Defense Nuclear Agency
  ATTN: SPTD
  ATTN: STSP
4 cy ATTN: TITL
4 cy ATTN: SPSS

Defense Technical Information Center
12 cy ATTN: DD

Field Command
Defense Nuclear Agency
  ATTN: FCT, W. Tyler
  ATTN: FCTO
  ATTN: FCTE, B. Johnson
  ATTN: FCTK, B. Ristvet
10 cy ATTN: FCTK, C. Keller
10 cy ATTN: FCTC, J. Lacomb

Field Command
Defense Nuclear Agency
Livermore Branch
  ATTN: FCPRL
  ATTN: Library

DoD-IDA Management Office
  ATTN: J. Statler

DEPARTMENT OF THE ARMY

U.S. Army Engineer Center
  ATTN: ATSEN-SV-L

U.S. Army Engr Waterways Exper Station
  ATTN: D. Day
  ATTN: J. Boa
  ATTN: J. Zelasko
  ATTN: W. Flathau
  ATTN: Rsch Center Lib
  ATTN: L. Ingram
  ATTN: P. Hadala
  ATTN: J. Jackson
  ATTN: J. Ehrgot

Harry Diamond Laboratories
Department of the Army
  ATTN: DRXDO-N-P, F. Wimenitz

Headquarters
Department of the Army
  ATTN: W. Murry

DEPARTMENT OF THE NAVY

Naval Construction Battalion Center
  ATTN: J. Allgood
  ATTN: Code L31

Naval Ordnance Station
  ATTN: Code 121

Naval Research Laboratory
  ATTN: Code 2627 for Code 1065
  ATTN: Code 2627 for Cont Branch

DEPARTMENT OF THE NAVY (Continued)

Chief of Naval Research
Department of the Navy
  ATTN: Technical Library

DEPARTMENT OF THE AIR FORCE

Air Force Weapons Laboratory
Air Force Systems Command
  ATTN: DE-I
  ATTN: DEV-G, J. Bratton
  ATTN: NTE, M. Plamondon
  ATTN: SES, R. Henning
  ATTN: Technical Library
  ATTN: DEX

Air Force Cambridge Research Labs
Air Force Systems Command
  ATTN: LWW, K. Thompson

DEPARTMENT OF ENERGY CONTRACTORS

Fenix & Scisson
  ATTN: F. Waltman
  ATTN: D. Townsend

Holmes & Narver, Inc
  ATTN: J. Calovini

Geotechnical Instrumentation & Grouting, Inc
  ATTN: Technical Library

Structural Mechanics Assoc
  ATTN: R. Kennedy

Reynolds Elec & Eng Co, Inc
  ATTN: FOD/DOD, H. Edwards

Los Alamos National Scientific Laboratory
  ATTN: J. McQueen
  ATTN: A. Davis
  ATTN: Report Library
  ATTN: F. App
  ATTN: R. Brownlee
  ATTN: B. Killian
  ATTN: L. Germain
  ATTN: J. House

Sandia National Laboratories
  ATTN: C. Gulick
  ATTN: C. Smith
  ATTN: C. Broyles
  ATTN: C. Mehl

Lawrence Livermore National Laboratory
  ATTN: J. Hearst
  ATTN: V. Wheeler
  ATTN: McKague
  ATTN: H. Rodean
  ATTN: R. Terhune
  ATTN: J. Shearer
  ATTN: B. Hudson

DEPARTMENT OF ENERGY

Department of Energy
Nevada Operations Office
    ATTN: R. Newman
    ATTN: Technical Library

OTHER GOVERNMENT AGENCIES

Bureau of Mines
    ATTN: T. Ricketts
    ATTN: T. Atchison

Department of the Interior
Bureau of Mines
    ATTN: G. Waddell/L. Obert

Department of the Interior
U.S. Geological Survey
    ATTN: R. Carroll
    ATTN: W. Twenhofel
    ATTN: B. Ellis

DEPARTMENT OF DEFENSE CONTRACTORS

Agbabian Associates
    ATTN: Technical Library
    ATTN: C. Bagge

Boeing Co
    ATTN: K. Fridell

General Electric Company—TEMPO
    ATTN: DASIAC

Shock Hydrodynamics, Inc
    ATTN: L. Zernow/K. Kreyenhagen

H-Tech
    ATTN: B. Hartenbaum

Pacific-Sierra Research Corp
    ATTN: H. Brode

Ken O'Brien and Associates, Inc
    ATTN: D. Donegan

DEPARTMENT OF DEFENSE CONTRACTORS (Continued)

Massachusetts Inst of Technology
    ATTN: W. Brace

Merritt CASES, Inc
    ATTN: J. Merritt

R & D Associates
    ATTN: R. Shaeffer
    ATTN: J. Lewis
    ATTN: P. Haas

SRI International
    ATTN: A. Florence
    ATTN: H. Lindberg

Pacifica Technology
    ATTN: D. Patch
    ATTN: J. Kent

Structural Mechanics Assoc
    ATTN: R. Kennedy

Systems, Science & Software, Inc
    ATTN: R. Duff
    ATTN: Technical Library
    ATTN: E. Peterson

Terra Tek, Inc
    ATTN: S. Green

TRW Defense & Space Sys Group
    ATTN: R1/2162, M. Schrader

Weidlinger Assoc, Consulting Engineers
    ATTN: M. Baron

University of Illinois
    ATTN: N. Newmark

University of Nevada
Desert Research Institute
    ATTN: P. Fenske
    ATTN: C. Case